Systematic Build-up of High-nuclearity Osmium–Mercury Clusters†

Lutz H. Gade,[a] Brian F. G. Johnson,[a] Jack Lewis,*[,a] Mary McPartlin*[,b] and Harold R. Powell[b]
[a] *University Chemical Laboratory, Lensfield Road, Cambridge CB2 1EW, UK*
[b] *School of Chemistry, The Polytechnic of North London, Holloway Road, London N7 8DB, UK*

The cluster dianion $[Os_{10}C(CO)_{24}]^{2-}$ **1** has been studied as a substrate for redox condensations with mercury(II) electrophiles. Its reaction with HgX_2 (X = Cl, Br or I) initially generates the halogenomercury-capped clusters $[Os_{10}C(CO)_{24}(HgX)]^-$ (X = Cl **2a**, Br **2b** or I **2c**) which undergo redistribution reactions in solution. This can be prevented by blocking one co-ordination site of the Hg atom with a CF_3 group, thus producing the stable monoanion $[Os_{10}C(CO)_{24}(HgCF_3)]^-$ **2d**. The structures of the $[N(PPh_3)_2]^+$ salt of **2b** and the $[PPh_4]^+$ salt of **2d** were established by single-crystal X-ray structure analysis. The reaction of **1** with 0.5–0.7 equivalent of $Hg(O_3SCF_3)_2$ leads to selective formation of the Hg-linked cluster dianion $[\{Os_{10}C(CO)_{24}\}_2Hg]^{2-}$ the structure of which was determined by X-ray crystallography as its $[N(PPh_3)_2]^+$ salt. The limits of this synthetic concept are set by the redox behaviour of the cluster. The cluster build-up achieved with **1** does not take place with its tetrahydrido analogue $[Os_{10}H_4(CO)_{24}]^{2-}$, which is instead oxidised by mercury salts to yield the radical monoanion.

A powerful method for the build-up of high-nuclearity carbonyl clusters is the reaction of anionic mono- or poly-nuclear carbonyl compounds with neutral or cationic ligand–metal fragments (redox condensation).[1] This concept was first established for mixed-metal systems where the coupling reaction of a neutral or anionic cluster with salts of Cu^I, Ag^I, Au^I, Hg^{II} or Tl^{III} leads to the build-up of extended cluster cores.[2] Recent detailed studies of this type of reaction have shown that the electronic properties of the metal and the steric requirements of the ligand co-ordinated to it can be used specifically to select one of the reaction pathways and cluster geometries feasible for the system.[3] There are a number of possible modes of attachment of the cationic fragment to the core. While in most cases these heterometal fragments adopt edge-bridging or face-capping positions on the otherwise unaltered cluster core, in species of higher nuclearity skeletal rearrangements reminiscent of those observed for a number of protonation reactions may occur.[4]

Low-valent transition-metal compounds containing one or more mercury atoms bound to the metal were among the first systems studied in the context of the conceptually new chemistry of metal–metal bonds in the early 1960s.[5] However, it was not until two decades later that the experience gained in these early studies was applied to cluster chemistry and since then an impressive variety of structures and reactions have been reported in this field. The main synthetic routes dominating this chemistry are (*a*) the reaction of a carbonyl cluster anion with a mercury or organomercury salt,[6] (*b*) the reaction of hydrido clusters with HgR_2 (R = phenyl or substituted aryl)[7] and (*c*) the oxidative addition of a mercury halide to a transition-metal cluster.[8] Other methods include the reactions of neutral clusters with metallic Hg or sodium amalgam, as used in the synthesis of the Pt–Hg clusters $[Hg\{Pt_3(2,6\text{-}MeC_6H_3NC)_6\}_2]$[9] and $[\{Pt_3Hg(CO)_3(PPhPr^i_2)_3\}_2]$.[10] A remarkable aspect of the chemical reactivity of clusters containing mercury-ligand fragments is the possibility of redistribution reactions in which capped/bridged and linked species are interconverted. These equilibria are sensitively dependent on the nature of the halide or alkyl/aryl ligand attached to the mercury and extensive studies of these redistribution reactions involving Ru_3 clusters have been published.[11]

High-nuclearity clusters offer a large range of possible reactive interactions with mercury salts, and to avoid complicated product mixtures it is necessary to focus as much attention on the solution properties of the mercury reagent as on the cluster itself. The most important properties of mercury compounds in this respect are their solubility in polar aprotic solvents, the degree of dissociation of the salt in these solvents and the strength of the mercury-ligand bond, in comparison with the M–Hg bonds to be formed. We have found that through an appropriate tuning of these properties it is possible to generate selectively either the capped/bridged or the linked cluster. Alternatively, the reaction may be directed towards more complex products by careful variation of the chosen stoichiometry.

Since its first synthesis[12] the cluster $[Os_{10}C(CO)_{24}]^{2-}$ **1** has been extensively studied, and its facile accessibility and chemical stability have made it an ideal model substrate for the manipulation of both the ligand shell and the metal core in a high-nuclearity cluster. In an early study it was found that the dianion **1** could be readily condensed with the metal electrophiles $[Au(PPh_3)]^+$ and $[Cu(MeCN)]^+$ yielding $[Os_{10}C(CO)_{24}(AuPPh_3)]^-$ **3a** and $[Os_{10}C(CO)_{24}(CuNCMe)]^-$ **3b** in which the heterometal fragment was shown to adopt edge-bridging and face-capping positions on the osmium core respectively.[13] However, with the exception of the Os–Au cluster $[Os_{10}Au_4C(CO)_{24}\{P(C_6H_{11})_3\}_3]$,[14] these cluster build-up reactions were limited to the addition of a single metal atom to the otherwise unaltered decaosmium core. Condensations leading to either heterometal-linked Os_{10} fragments or more complicated mixed-metal cores have so far not been achieved with either copper(I) or gold(I) reagents. We here report the reactivity of $[Os_{10}C(CO)_{24}]^{2-}$ towards a variety of mercury(II) reagents, the systematic build-up of high-nuclearity osmium–mercury clusters with novel core geometries and their structural characterisation by X-ray crystallography.[15]

† *Supplementary data available:* see Instructions for Authors, *J. Chem. Soc., Dalton Trans.*, 1992, Issue 1, pp. xx–xxv.

Table 1 Spectroscopic data for the Os–Hg clusters

Compound	IR[a]/cm^{-1}	MS[b] *m/z*	^{13}C NMR(δ)[c]
1 $[Os_{10}C(CO)_{24}]^{2-}$[d]	2035s, 1987s	2889 (2888)	178.2, 189.9
2a $[Os_{10}C(CO)_{24}(HgCl)]^-$	2093w, 2064vs, 2013s	2822 (2823)	174.0, 183.7
2b $[Os_{10}C(CO)_{24}(HgBr)]^-$	2093w, 2064vs, 2013s	2865 (2867)	174.1, 183.8
2c $[Os_{10}C(CO)_{24}(HgI)]^-$	2092w, 2063vs, 2013s	2913 (2915)	174.2, 183.9
2d $[Os_{10}C(CO)_{24}(HgCF_3)]^-$	2092w, 2063vs, 2014s	2858 (2857)	174.4, 184.1
2e $[Os_{10}C(CO)_{24}\{HgMo(CO)_3(cp)\}]^-$	2088w, 2058vs, 2008s, 1991 (sh) 1921w, 1895w	3033 (3034)	*e*
2f $[Os_{10}C(CO)_{24}\{HgFe(CO)_2(cp)\}]^-$	2086w, 2057vs, 2006s, 1990 (sh), 1940w	—	—
2g $[Os_{10}C(CO)_{24}(HgO_2CCF_3)]^-$	2093w, 2064vs, 2013s	—	—
4 $[\{Os_{10}C(CO)_{24}\}_2Hg]^{2-}$	2083w, 2060vs, 2050 (sh), 2006s	*ca.* 5380 (5377)	*e*
7 $[Os_{10}H_4(CO)_{24}]^{2-}$[f]	2076vw, 2035vs, 1996 (sh), 1986s	2580 (2580)	175.8, 192.9
7a $[Os_{10}H_4(CO)_{24}]^-$[g]	2092vw, 2056vs, 2050 (sh) 2015 (sh), 2009s	2580 (2580)	—
8 $[Os_{10}H_4(CO)_{24}(HgO_2CCF_3)]^-$	2095w, 2063vs, 2050 (sh) 2022 (sh), 2014s	—	—
9 $[Os_{10}H_4(CO)_{24}(HgCF_3)]^-$	2093w, 2063vs, 2050 (sh) 2020 (sh), 2012s	2847 (2849)	—

[a] Recorded in CH_2Cl_2. [b] Negative ion FAB mass spectra: most abundant isotopomer found (simulated). [c] Recorded in CD_2Cl_2 at 295 K, $SiMe_4$ reference. [d] First reported in ref. 12. [e] Broad spectral features due to chemical exchange; see ref. 16. [f] IR and MS data first reported in ref. 17. [g] IR and MS data first reported in ref. 18.

Results and Discussion

Capping of $[Os_{10}C(CO)_{24}]^{2-}$ **1** *with* HgY *Fragments* [Y = Cl, Br, I, CF_3, $Mo(CO)_3(cp)$ *or* $Fe(CO)_2(cp)$; cp = η-C_5H_5] **2a–2f**.—Reaction of the $N(PPh_3)_2^+$ salt of cluster **1** with 1 equivalent of HgX_2 (X = Cl, Br or I) almost immediately leads to the formation of the halogenomercury-capped clusters [equation (1)]. The red solutions of **1** turn deep brown and

$$[N(PPh_3)_2]_2[Os_{10}C(CO)_{24}] + HgX_2 \longrightarrow [N(PPh_3)_2][Os_{10}C(CO)_{24}(HgX)] + [N(PPh_3)_2]X \quad (1)$$
X = Cl **2a**, Br **2b**, or I **2c**

their infrared spectra reflect the change of the overall charge of the cluster in this reaction by a shift of the ν(CO) absorption bands to higher wavenumbers (Table 1). Additionally, the now reduced symmetry of the cluster manifests itself in the appearance of a third weak band along with the two intense absorptions.

Solutions of compounds **2a–c** are stable for at least 4–5 h and can be conveniently studied spectroscopically during that time, but over a period of days redistribution reactions occur leading to mixtures of different species. This propensity to undergo redistribution reactions in solution made it desirable to investigate the reactions in more detail. Since it seemed likely that one of the initial reaction steps in the thermal degradation of these compounds was the dissociation of the halide, particular attention was focused on this co-ordination site of the mercury atom. Blocking it by the strongly electron-withdrawing CF_3 group effects a complete suppression of the redistribution under the reaction conditions. The monoanion $[Os_{10}C(CO)_{24}(HgCF_3)]^-$ **2d** is generated by reaction of **1** with 1 equivalent of $Hg(CF_3)(O_2CCF_3)$ and appears to be stable in solution even over periods of weeks. The similarity of the ν(CO) band pattern in the IR spectrum of **2d** to that observed for **2a–c** indicated a related core geometry.

Stabilisation of the mercury-capped species could also be achieved by co-ordination of the mercury atom to the mononuclear transition-metal fragment $Mo(CO)_3(cp)$. The Hg-$[Mo(CO)_3(cp)]$ group had previously been attached to a number of low-nuclearity clusters and was found to generate stable mixed-metal systems, such as $[Ru_3(C_6H_9)(CO)_9\{HgMo(CO)_3(cp)\}]$,[19] $[Fe_4(CO)_{13}\{HgMo(CO)_3(cp)\}]^-$ [20] as well as $[FeCo_3(CO)_{12}\{HgMo(CO)_3(cp)\}]$.[6d] The formation of $[Os_{10}C(CO)_{24}\{HgMo(CO)_3(cp)\}]^-$ **2e** from **1** and $[Mo(CO)_3(cp)(HgCl)]$ in the presence of $TlPF_6$ can be readily monitored by infrared spectroscopy. In the IR spectrum of **2e** the ν(CO) bands for the μ_3-capped (or μ-bridged) cluster fragment (2088w, 2058vs and 2008s cm^{-1}) are clearly separated from those of the $Mo(CO)_3(cp)$-fragment [1991 (sh), 1921w and 1895w]. The analogous $(cp)(OC)_2FeHg$-bridged system $[Os_{10}C(CO)_{24}\{HgFe(CO)_2(cp)\}]^-$ **2f** was synthesised by condensation of **1** with $[Fe(CO)_2(cp)(HgCl)]$ in the presence of $TlPF_6$. As was also found by Shriver and co-workers[20] for $[Fe_4(CO)_{13}\{HgFe(CO)_3(cp)\}]^-$, the FeHg-bridged cluster **2f** is considerably less stable than the corresponding molybdenum compound and slowly decomposed in solution. The absence of the molecular ion in its negative-ion fast atom bombardment (FAB) mass spectrum may also be attributed to the thermal instability of the system (Table 1).

The Crystal Structures of Compounds **2b** *and* **2d**.—Crystals of the halogenomercury clusters **2a–2c** suitable for X-ray diffraction studies were difficult to obtain due to the redistribution reactions they undergo in solution. Eventually, good crystals were obtained of the $[N(PPh_3)_2]^+$ salt of the bromomercury cluster **2b** and X-ray structure analyses of this and of the rather weakly diffracting crystal of the $[PPh_4]^+$ salt of the trifluoromethylmercury monoanion **2d** confirmed that the two clusters have similar metal frameworks. The overall structures of **2b** and **2d** are shown in Fig. 1(*a*) and 1(*b*) respectively, and selected bond lengths and angles are compared in Table 2.

The basic arrangement of the metal core reported[12] for the dianion $[Os_{10}C(CO)_{24}]^{2-}$ **1** is maintained in the structures of **2b** and **2d**, with the mercury atom in each adopting a μ_3 site bridging a face of one of the four capping tetrahedra of the Os_{10} unit. The Os_3 triangle bridged by the mercury atom is enlarged in both structures; in **2b** the bridged Os–Os distances are in the range 2.925–3.138, mean 3.006 Å, and in **2d** the range is 2.811–3.054, mean 2.973 Å (corresponding ranges for the remaining Os–Os distances are 2.728–2.936 for **2b** and 2.728–2.927 Å for **2d**). The carbonyl ligands are terminal and maintain the same overall distribution as in the precursor dianion **1**, with two on each of the osmium atoms of the central octahedron and three on each of the capping osmium atoms. The presence of the heteroatom perturbs the highly symmetrical carbonyl array observed in the dianion **1** and in Table 2 the relevant osmium carbonyl angles reported for **1**[12] are compared with the corresponding values in the vicinity of the mercury atoms in **2b** and **2d**.

It can be seen from Fig. 1(*a*) and 1(*b*) that in the crystal

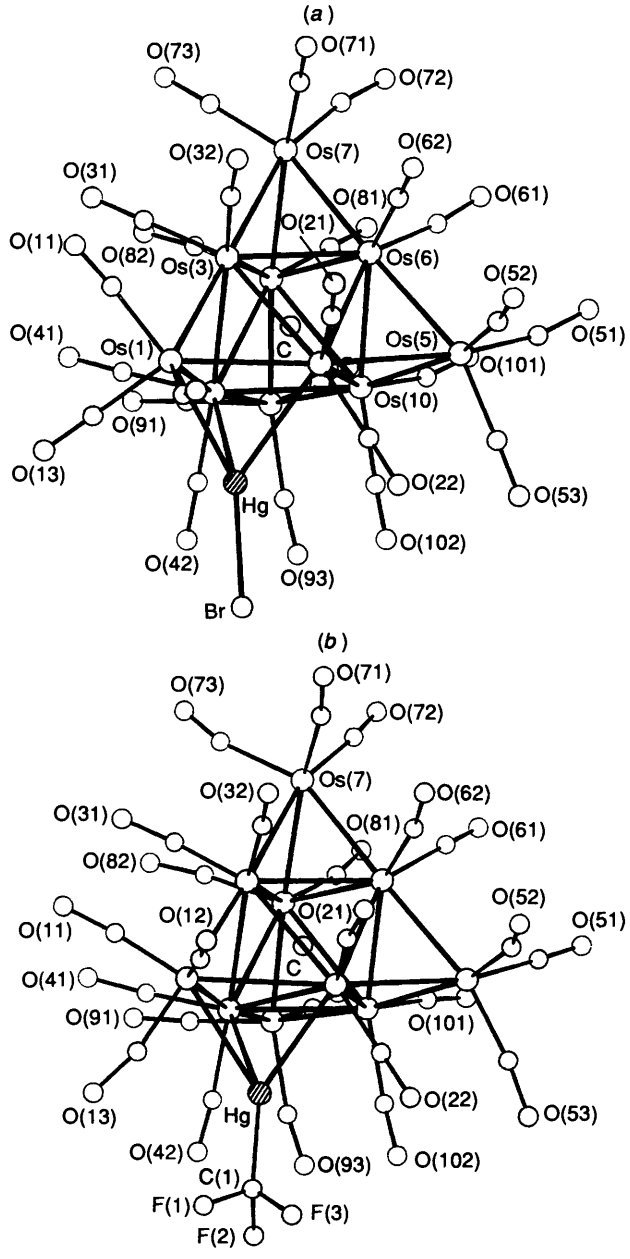

Fig. 1 The molecular structures of (*a*) $[Os_{10}C(CO)_{24}(HgBr)]^-$ **2b** and (*b*) $[Os_{10}C(CO)_{24}(HgCF_3)]^-$ **2d**. The principal bond distances and angles are listed in Table 2

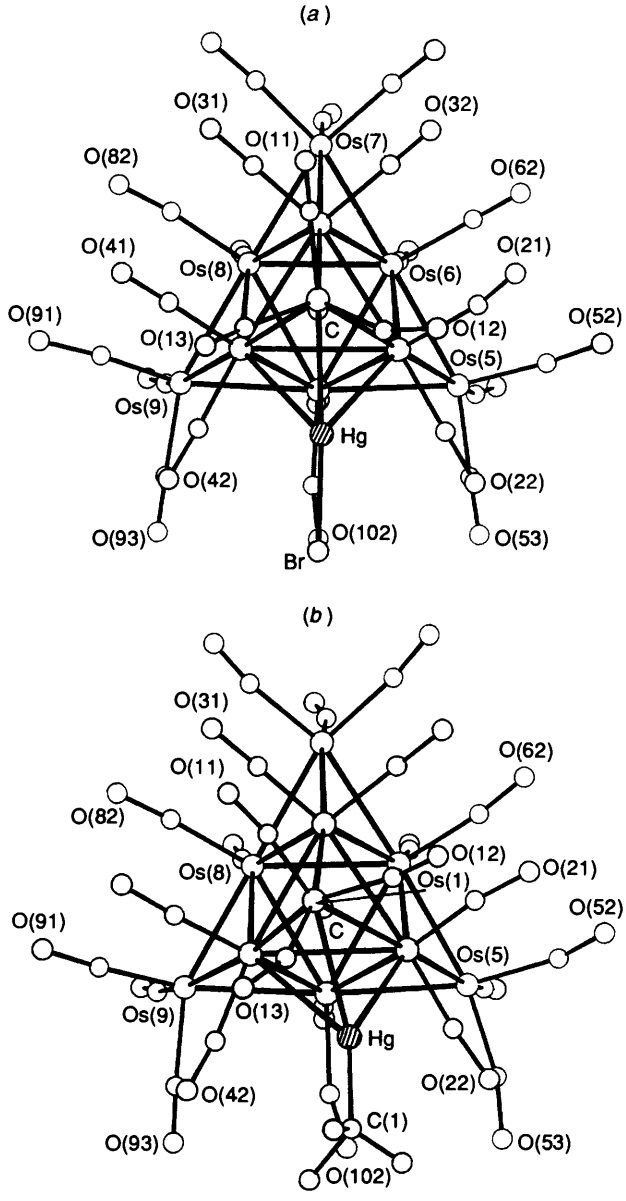

Fig. 2 The molecular structures of (*a*) compound **2b** and (*b*) **2d** viewed along the three-fold axis of the Os_{10} tetrahedron through the vertex to which the mercury fragment is attached in order to illustrate the distortion of the vertex $Os(CO)_3$ group as a consequence of the steric requirements of the mercury atom

structures there is a distinct asymmetry in the immediate environment of the μ_3-mercury atoms of **2b** and **2d**, the details differing between the two monoanions. For example, the distances from the mercury atoms show small but significant inequalities; in **2b** there are two rather long distances [Hg–Os(4) 2.924(2) and Hg–Os(2) 2.850(2) Å] and one short [Hg–Os(1) 2.730(2) Å] whereas in **2d** there is a different pattern with the Hg–Os(4) distance of 3.111(5) Å being very long and the two remaining distances Hg–Os(1) and Hg–Os(2) being much shorter, 2.786(4) and 2.733(4) Å respectively.

Marked differences in the two monoanions are also evident in the orientations adopted by the carbonyl ligands in accommodating the large mercury atoms. This can be seen most readily in Fig. 2(*a*) and 2(*b*) which show corresponding views of **2b** and **2d** respectively on to the capping atom Os(1). In the bromo-substituted cluster **2b** [Fig. 2(*a*)] the carbonyl ligands on Os(1) are nearly eclipsed with respect to the capping Os–Os bonds, having rotated away from the approximately staggered configuration observed in $[Os_{10}C(CO)_{24}]^{2-}$ **1** and in the remaining caps of **2b**; as a result there are four relatively short contacts between the Hg atom and the carbonyl-ligands C(12) 3.00, C(13) 3.07, C(22) 2.81 and C(42) 2.79 Å. In contrast Fig. 2(*b*) shows that in the trifluoromethyl cluster **2d** the carbonyl ligands on Os(1) are only slightly rotated from the staggered conformation and give rise to three short contacts between the Hg atom and carbonyl ligands, C(13) 2.73, C(22) 2.61 and C(42) 2.93 Å. Closer carbonyl-mercury contacts are avoided by a marked 'pushing back' of the carbonyls surrounding the mercury sites (Table 2); for example, the C(42)–Os(4)–Os(3) and C(22)–Os(2)–Os(3) angles of 167(1) and 170.2(9)° in **2b** and 163(2) and 174(2)° in **2d** respectively are much larger than the corresponding values of 148(1) and 143.3(8)° in **1**.

Although crystals suitable for a single-crystal X-ray structure analysis could not be obtained from either compound **2e** or **2f**, it is possible to propose reasonable structures. On the basis of the core geometries found for the $(cp)(OC)_xMHg$-functionalised (M = Mo, x = 3; M = Fe, x = 2) Ru_3 and Fe_4 clusters mentioned above and the considerably higher steric demand of

Table 2 Comparison of selected bond lengths (Å) and angles (°) for compounds **2b** and **2d**

	2b	**2d**		**2b**	**2d**
Os(1)–Os(2)	2.955(2)	3.054(4)	Os(4)–Os(10)	2.906(2)	2.874(4)
Os(1)–Os(3)	2.728(2)	2.732(4)	Os(5)–Os(6)	2.734(2)	2.739(4)
Os(1)–Os(4)	2.925(2)	2.811(4)	Os(5)–Os(10)	2.761(2)	2.754(4)
Os(2)–Os(3)	2.935(2)	2.926(4)	Os(6)–Os(7)	2.760(2)	2.776(4)
Os(2)–Os(4)	3.138(2)	3.054(4)	Os(6)–Os(8)	2.838(2)	2.841(4)
Os(2)–Os(5)	2.877(2)	2.892(4)	Os(6)–Os(10)	2.867(2)	2.895(4)
Os(2)–Os(6)	2.851(2)	2.865(4)	Os(7)–Os(8)	2.756(2)	2.763(4)
Os(2)–Os(10)	2.916(2)	2.927(4)	Os(8)–Os(9)	2.735(2)	2.728(4)
Os(3)–Os(4)	2.936(2)	2.927(4)	Os(8)–Os(10)	2.866(2)	2.877(4)
Os(3)–Os(6)	2.824(2)	2.831(4)	Os(9)–Os(10)	2.757(2)	2.789(4)
Os(3)–Os(7)	2.859(2)	2.847(4)	Os(1)–Hg	2.730(2)	2.786(4)
Os(3)–Os(8)	2.826(2)	2.821(4)	Os(2)–Hg	2.850(2)	2.733(4)
Os(4)–Os(8)	2.861(2)	2.874(4)	Os(4)–Hg	2.924(2)	3.111(5)
Os(4)–Os(9)	2.859(2)	2.838(4)			

The heterometallic capping group

	2b	**2d**		**2b**	**2d**
Hg–Os(1)–Os(2)	60.0(1)	55.6(1)	Hg–Os(4)–Os(3)	100.8(1)	98.1(1)
Hg–Os(1)–Os(3)	111.7(1)	111.5(1)	Hg–Os(4)–Os(8)	142.2(1)	140.2(1)
Hg–Os(1)–Os(4)	62.2(1)	67.5(1)	Hg–Os(4)–Os(9)	127.9(1)	131.7(1)
Hg–Os(2)–Os(1)	56.1(1)	57.2(1)	Hg–Os(4)–Os(10)	90.7(1)	90.6(1)
Hg–Os(2)–Os(3)	102.7(1)	107.4(1)	Os(2)–Hg–Os(1)	63.9(1)	67.2(1)
Hg–Os(2)–Os(4)	58.2(1)	64.8(1)	Os(4)–Hg–Os(1)	62.2(1)	56.6(1)
Hg–Os(2)–Os(5)	127.2(1)	127.2(1)	Os(4)–Hg–Os(2)	65.8(1)	62.6(1)
Hg–Os(2)–Os(6)	144.4(1)	151.8(1)	Br/C(1)–Hg–Os(1)	147.9(2)	139(3)
Hg–Os(2)–Os(10)	92.0(1)	97.5(1)	Br/C(1)–Hg–Os(2)	139.6(2)	150(3)
Hg–Os(4)–Os(1)	55.6(1)	55.8(1)	Br/C(1)–Hg–Os(4)	139.2(2)	139(3)
Hg–Os(4)–Os(2)	55.9(1)	52.6(1)			

OC–Os–Os and OC–Os–CO compared to those in the dianion **1**

	2b	**2d**	**1**		**2b**	**2d**	**1**
C(11)–Os(1)–Os(2)	129.8(9)	149(3)	159.3(9)	C(31)–Os(3)–Os(8)	93.0(7)	90(2)	97.9(9)
C(11)–Os(1)–Os(3)	79.6(9)	90(3)	99.5(8)	C(32)–Os(3)–Os(1)	93.3(9)	96(2)	89.4(8)
C(11)–Os(1)–Os(4)	125.3(9)	113(3)	101.9(9)	C(32)–Os(3)–Os(2)	98(1)	95(2)	97.8(6)
C(12)–Os(1)–Os(2)	90(2)	91(2)	98.7(8)	C(32)–Os(3)–Os(4)	154.1(9)	152(2)	147.1(7)
C(12)–Os(1)–Os(3)	133(2)	106(2)	102.4(9)	C(32)–Os(3)–Os(6)	96(1)	93(2)	98.9(7)
C(12)–Os(1)–Os(4)	140(2)	153(2)	158.8(9)	C(32)–Os(3)–Os(7)	87.2(9)	87(2)	92.1(8)
C(13)–Os(1)–Os(2)	140(1)	123(2)	101.9(9)	C(32)–Os(3)–Os(8)	144.2(9)	143(2)	149.7(8)
C(13)–Os(1)–Os(3)	134(1)	166(2)	160.4(10)	C(41)–Os(4)–Os(1)	85.3(8)	83(2)	90.9(8)
C(13)–Os(1)–Os(4)	90(1)	105(2)	101.7(11)	C(41)–Os(4)–Os(2)	139.9(9)	143(2)	148.3(8)
C(21)–Os(2)–Os(1)	88(1)	88(2)	91.1(7)	C(41)–Os(4)–Os(3)	89.1(8)	93(2)	97.3(7)
C(21)–Os(2)–Os(3)	91(1)	88(2)	100.0(6)	C(41)–Os(4)–Os(8)	94.1(8)	95(2)	97.9(8)
C(21)–Os(2)–Os(4)	142(1)	140(2)	149.1(6)	C(41)–Os(4)–Os(9)	99.1(8)	94(2)	92.5(8)
C(21)–Os(2)–Os(5)	98(1)	100(2)	90.2(7)	C(41)–Os(4)–Os(10)	150.8(8)	150(2)	149.0(4)
C(21)–Os(2)–Os(6)	93.8(9)	93(2)	99.3(7)	C(42)–Os(4)–Os(1)	111(1)	106(2)	89(1)
C(21)–Os(2)–Os(10)	150(1)	150(2)	148.3(7)	C(42)–Os(4)–Os(2)	116(1)	113(2)	98(1)
C(22)–Os(2)–Os(1)	115.0(9)	119(2)	87.3(8)	C(42)–Os(4)–Os(3)	167(1)	163(2)	148(1)
C(22)–Os(2)–Os(3)	170.2(9)	174(2)	143.3(8)	C(42)–Os(4)–Os(8)	135(1)	139(2)	149(1)
C(22)–Os(2)–Os(4)	119.5(8)	119(2)	91.1(8)	C(42)–Os(4)–Os(9)	78(1)	82(2)	91(1)
C(22)–Os(2)–Os(5)	74.6(9)	71(2)	93.3(8)	C(42)–Os(4)–Os(10)	99(1)	99(2)	98(1)
C(22)–Os(2)–Os(6)	131.4(9)	128(2)	147.7(9)	C(12)–Os(1)–C(11)	94(2)	90(3)	94(1)
C(22)–Os(2)–Os(10)	99.2(8)	96(2)	93.7(10)	C(13)–Os(1)–C(11)	89(2)	87(3)	90(1)
C(31)–Os(3)–Os(1)	94.7(7)	96(2)	90.2(8)	C(13)–Os(1)–C(12)	92(2)	88(3)	94(1)
C(31)–Os(3)–Os(2)	155.7(7)	159(2)	147.2(7)	C(22)–Os(2)–C(21)	88(1)	92(3)	95(1)
C(31)–Os(3)–Os(4)	97.7(7)	101(2)	96.6(7)	C(32)–Os(3)–C(32)	92(1)	95(3)	91(1)
C(31)–Os(3)–Os(6)	141.7(7)	137(2)	149.4(8)	C(42)–Os(4)–C(41)	91(1)	88(2)	91(1)
C(31)–Os(3)–Os(7)	85.0(7)	80(2)	92.6(8)				

the $(cp)(OC)_xM$ group in comparison to a halide, the mercury fragment probably adopts a μ-edge-bridging position similar to that of the Ph_3PAu fragment in $[Os_{10}C(CO)_{24}(AuPPh_3)]^-$.[13]

^{13}C NMR Spectroscopy of Compounds **2a**–**2d** *in Solution.*—The solid state structures of compound, **2b** and **2d** have approximately C_s symmetry and for a rigid molecule a pattern of 10–14 resonances in the ^{13}C NMR spectra would be anticipated. The spectra of **2a**–**2d** observed at 300 K, however, consist of only two signals of almost equal intensity, *i.e.* a pattern which is identical to that of the starting material, albeit shifted to higher field by *ca.* 5 ppm (Table 1). A possible interpretation is that the system is fluxional at 300 K with the F_3CHg^+ fragment rapidly moving over the four faces of the Os_{10} tetrahedron, thereby generating the overall T_d symmetry on the NMR time-scale. Low-temperature studies confirm this view and a full account of the solution properties of these clusters is given in the following paper.[16]

Redistribution Reactions of Compounds **2a**–**2c** *in Solution.*—The inertness of compound **2d** with respect to redistribution highlights the importance of the nature of the Hg–Y bond for the overall stability of the mercury-capped cluster. In order to

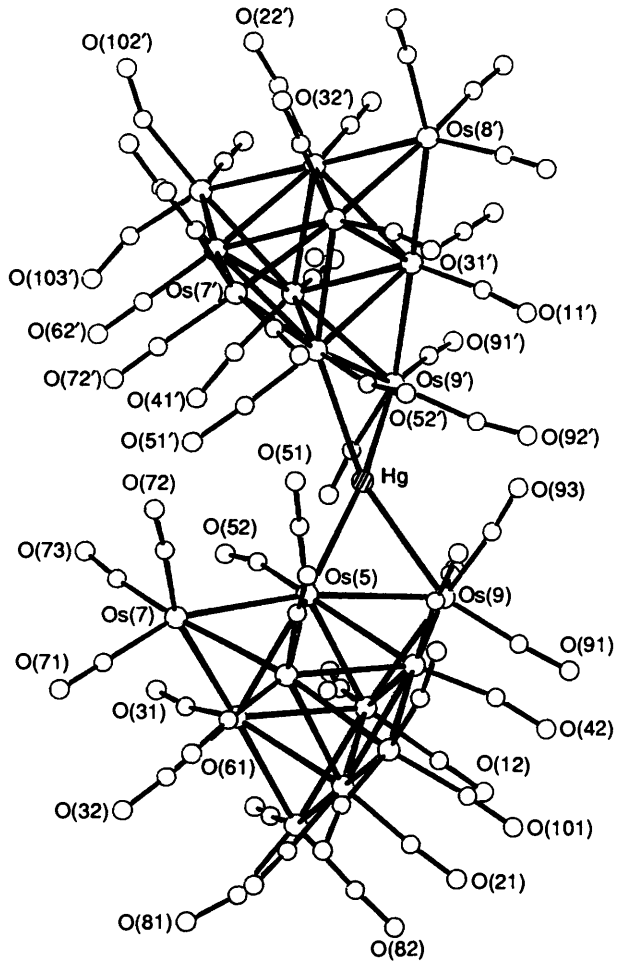

Fig. 3 The molecular structure of $[\{Os_{10}C(CO)_{24}\}_2Hg]^{2-}$ **4**. The principal bond distances and angles are listed in Table 3

Table 3 Selected bond lengths (Å) and angles (°) for compound **4**

Os(1)–Os(2)	2.851(2)	Os(1)–Os(3)	2.869(2)
Os(1)–Os(4)	2.911(2)	Os(1)–Os(5)	2.898(2)
Os(1)–Os(8)	2.800(2)	Os(1)–Os(9)	2.775(2)
Os(2)–Os(4)	2.886(2)	Os(2)–Os(6)	2.881(2)
Os(2)–Os(8)	2.771(2)	Os(2)–Os(10)	2.744(3)
Os(2)–Os(3)	2.856(2)	Os(3)–Os(5)	2.886(2)
Os(3)–Os(6)	2.902(2)	Os(3)–Os(7)	2.750(2)
Os(3)–Os(8)	2.807(2)	Os(4)–Os(5)	2.929(2)
Os(4)–Os(6)	2.835(2)	Os(4)–Os(9)	2.772(2)
Os(4)–Os(10)	2.817(2)	Os(5)–Os(6)	2.916(2)
Os(5)–Os(7)	2.925(2)	Os(5)–Os(9)	2.990(2)
Os(6)–Os(7)	2.764(2)	Os(6)–Os(10)	2.808(2)
Os(5)–Hg	2.866(2)	Os(9)–Hg	2.902(2)
Os–C (carbonyl)		1.75(4)–1.93(5)	
Os–C (carbide)		1.99(3)–2.08(3)	
C–O (carbonyl)		1.09(4)–1.28(4)	

Hg–Os(5)–Os(1)	106.5(1)	Hg–Os(5)–Os(3)	150.6(1)
Hg–Os(5)–Os(4)	106.5(1)	Hg–Os(5)–Os(6)	149.3(1)
Hg–Os(5)–Os(7)	131.4(1)	Hg–Os(5)–Os(9)	59.4(1)
Hg–Os(9)–Os(1)	108.9(1)	Hg–Os(9)–Os(4)	109.9(1)
Hg–Os(9)–Os(5)	58.2(1)	Os(9)–Hg–Os(5)	62.4(1)
C(51)–Os(5)–Os(1)	158(1)	C(51)–Os(5)–Os(3)	131(1)
C(51)–Os(5)–Os(4)	98(1)	C(51)–Os(5)–Os(6)	83(1)
C(51)–Os(5)–Os(7)	77(1)	C(51)–Os(5)–Os(9)	108(1)
C(52)–Os(5)–Os(1)	99(1)	C(52)–Os(5)–Os(3)	89(1)
C(52)–Os(5)–Os(4)	156(1)	C(52)–Os(5)–Os(6)	139(1)
C(52)–Os(5)–Os(7)	84(1)	C(52)–Os(5)–Os(9)	104(1)
C(91)–Os(9)–Os(1)	93(1)	C(91)–Os(9)–Os(4)	91(1)
C(91)–Os(9)–Os(5)	147(1)	C(92)–Os(9)–Os(1)	98(1)
C(92)–Os(9)–Os(4)	161(1)	C(92)–Os(9)–Os(5)	113(1)
C(93)–Os(9)–Os(1)	158(1)	C(93)–Os(9)–Os(4)	95(1)
C(93)–Os(9)–Os(5)	109(1)	C(52)–Os(5)–C(51)	101(2)
C(93)–Os(9)–C(91)	89(2)	C(93)–Os(9)–C(92)	103(2)
C(92)–Os(9)–C(91)	88(2)	Os(5)–Hg–Os(9′)	160.2(1)
Os(5)–Hg–Os(5′)	124.1(1)	Os(9)–Hg–Os(9′)	118.7(1)

obtain more details about the chemical reactivity of these systems the degradation of solutions of **2a**–**2c** was monitored by infrared spectroscopy over a period up to 6 weeks and the reaction products identified as soon as no further spectroscopic change could be observed. At ambient temperatures the reaction was complete after *ca.* 2 weeks for **2a** and after 3–4 weeks for **2b** and **2c**. In all cases substantial amounts of the starting material (*ca.* 40%) were still present in the reaction mixture; other components were **1** (*ca.* 15%), $[\{Os_{10}C(CO)_{24}\}_2Hg]^{2-}$ **4** (< 10%) and $[Os_{18}Hg_3C_2(CO)_{42}]^{2-}$ **5** (up to 20%)[19] which were identified by IR and mass spectrometry. A number of minor fractions could not be identified. While the formation of **4** is explicable in terms of an ordinary redistribution reaction, the generation of the trimercury species **5** suggests the competition of at least one additional reaction pathway.

Reaction of Compound **1** *with* $Hg(O_2CCF_3)_2$.—While the degradation of compounds **2a**–**2c** takes up to 4 weeks this process can be substantially enhanced by treating **1** with 1 molar equivalent of $Hg(O_2CCF_3)_2$. Initially, the capped cluster $[Os_{10}C(CO)_{24}(HgO_2CCF_3)]^-$ **2g** is generated as determined by IR spectroscopy. The subsequent reaction can be conveniently monitored by either IR or ^{13}C NMR spectroscopy which show the formation of substantial amounts of **5** within the first 2–4 min. After 5–7 d no further spectroscopic change is observed. The product distribution resembles that found for **2a**–**2c** albeit with a decreased proportion of **2g** (< 10%) and **1** (< 5%) and significantly larger amounts of **4** (30–40%). This probably reflects the fact that the trifluoroacetate ligand is more easily displaced through nucleophilic attack by the dianion **1** than the halides which implies that the equilibrium (2) is shifted

$$\underset{\mathbf{2g}}{[Os_{10}C(CO)_{24}(HgO_2CCF_3)]^-} + \underset{\mathbf{1}}{[Os_{10}C(CO)_{24}]^{2-}} \overset{-CF_3CO_2^-}{\rightleftharpoons} \underset{\mathbf{4}}{[\{Os_{10}C(CO)_{24}\}_2Hg]^{2-}} \quad (2)$$

towards **4**. The generation of **4** can, however, be completely suppressed if **1** is treated with 1.5–1.7 equivalents of the trifluoroacetate, which leads to the almost exclusive generation of **5** (yields > 90%). The chemistry associated with this reaction has been exhaustively studied and is reported in ref. 21.

Selective Synthesis and Structure of $[\{Os_{10}C(CO)_{24}\}_2Hg]^{2-}$ **4**.—The observed dependence of the proportion of compound **4** generated in the redistribution reactions on the lability of the ligand co-ordinated to the mercury atom prompted attempts selectively to generate this species. This could be conveniently achieved by treating **1** with 0.5–0.7 molar equivalent of the highly dissociated $Hg(O_3SCF_3)_2$. At ambient temperatures the generation of the monomercury-linked cluster dianion takes place immediately and it proved impossible to detect a capped intermediate under these reaction conditions. The formulation $[Os_{20}HgC_2(CO)_{42}]^{2-}$ **4** was established by FAB mass spectroscopy, and the ν(CO) absorption band pattern in the IR spectrum (Table 1) was also consistent with the formation of the dianionic Hg-linked cluster. A single-crystal X-ray structure analysis of **4** as its $[N(PPh_3)_2]^+$ salt confirmed the formulation and established the cluster structure depicted in Fig. 3; selected bond distances and angles are listed in Table 3. The 21-metal-atom core consists of two $Os_{10}C(CO)_{24}$ units linked by a single mercury atom in a doubly bridging configuration with a crystallographic C_2 axis through the mercury centre. The Hg

atom is four-co-ordinate with geometry intermediate between tetrahedral and square planner. The dihedral angle between the planes Os(5)–Os(9)–Hg and Os(5′)–Os(9′)–Hg is 38.43°. This kind of arrangement of two cluster fragments has previously been reported for a number of systems derived from trinuclear cluster anions[7,22] with the corresponding dihedral angles between the planes M(1)–M(2)–Hg and M(1′)–M(2′)–Hg ranging from 27.6° for $[\{Ru_3(CO)_{10}(NO)\}_2Hg]^{2-}$[22a] to 71.9° for $[\{Fe_2Rh(\mu_3\text{-}COMe)(CO)_7(C_5H_5)\}_2Hg]$.[7]

The μ site adopted by the linking Hg atom in $[\{Os_{10}C(CO)_{24}\}_2Hg]^{2-}$ **4** contrasts with the slightly asymmetric μ_3 mode adopted by the capping Hg atoms in the monoanions **2b** and **2d**, a difference which is readily explained by steric factors associated with the proximity of the two linked $Os_{10}C(CO)_{24}$ units in **4**. The closest approach of these two symmetry-related parts of the cluster is between the two carbonyl ligands O(51) ··· C(52′) 2.88 Å, a distance which is of the same order as the minimum interionic contact between carbonyl ligands involving two adjacent dianions related by the crystallographic inversion centre [O(12) ··· O(11″) 2.84 and O(92) ··· C(82″) 3.07 Å]. Much shorter and more unfavourable carbonyl interactions between the two halves of the dianion **4** would have been difficult to avoid had there been a μ_3-linking atom.

The structure of the Hg-linked cluster **4** may be compared with that of $[Os_{10}C(CO)_{24}Au\{AuP(C_6H_{11})\}_3]$ **6**,[14] the only other example of linkage of the large $[Os_{10}C(CO)_{24}]^{2-}$ dianion to a second cluster unit, and also with the monoanion $[Os_{10}C(CO)_{24}(\mu\text{-}AuPPh_3)]^-$ **3a**.[13] The unique linking gold atom in **6** and the $AuPPh_3$ group in **3a** each adopt a μ site spanning one cap of the Os_{10} framework. The angle subtended by the bridging atom, Os–Au–Os, is 65.6° in **6** and 63.5° in **3a**, both slightly larger than the corresponding μ-bridging Os(5)–Hg–Os(9) angle of 62.4° in **4**. The steady slight decrease in these angles is largely related to a corresponding increase in the mean osmium–heterometal distances in the three compounds of 2.784, 2.816 and 2.884 Å for **6**, **3a** and **4** respectively. In each of the three structures the bridged Os–Os distance shows the characteristic lengthening usually associated with a μ-heterometal fragment and is the longest Os–Os bond in the structures of **4** (2.990 Å), **6** (3.025 Å) and **3a** (2.962 Å).

In the Hg-linked cluster **4** and the monoanion **3b** the heteroatom adopts a fairly symmetrical position relative to the tetrahedral Os_{10} framework. In **4** the angles between the planes through the bridging unit Os(5)–Hg–Os(9) and the two adjacent triangular faces Os(1)–Os(5)–Os(9) and Os(4)–Os(5)–Os(9) are almost equal being 142.6 and 144.4° respectively, similar to the related angles of 142.0 and 144.4° in **3a**.[13] In contrast, in the Au-linked cluster $[Os_{10}C(CO)_{24}Au\{AuP(C_6H_{11})\}_3]$ **6** the unique μ-Au linking atom is markedly more asymmetric; the interplane angles between the bridging Os(1)–Au–Os(2) unit and the adjacent triangular faces Os(1)–Os(2)–Os(3) and Os(1)–Os(2)–Os(4) were found to be 135.9 and 150.0° respectively.[14]

The use of $Hg(O_3SCF_3)_2$ as a reagent in the reaction with compound **1** at ambient temperatures and various stoichiometries effects a complete suppression of the reaction pathway leading to $[Os_{18}Hg_3C_2(CO)_{42}]^{2-}$ **5**, a cluster in which the tetracapped-octahedral metal core of **1** has been decapped to afford an overall metal framework with two $Os_9C(CO)_{21}$ units fused together by an Hg_3 triangle. This observation highlights the importance of the halide and trifluoroacetate ligands, especially with regard to their reactivity as nucleophiles towards the metal framework activated by the capping mercury fragment. The decisive properties of the triflate (O_3SCF_3) anion which make the generation of **4** a highly selective process while suppressing the decapping of the metal core of the starting material are two-fold: (*a*) its very low nucleophilicity and (*b*) the ease with which it is displaced from a Hg atom already attached to the cluster core, thus shifting the analogous equilibrium to that represented in equation (2) towards the linked cluster **4**.

Another way of selectively achieving the latter using compounds **2a**–**2c** as intermediates is the addition of a non-oxidising halide acceptor like $TlPF_6$, *e.g.* as in equation (3). This

$$\underset{\mathbf{2b}}{[Os_{10}C(CO)_{24}(HgBr)]^-} + \underset{\mathbf{1}}{[Os_{10}C(CO)_{24}]^{2-}} \xrightarrow[-TlBr]{+TlPF_6} \underset{\mathbf{4}}{[\{Os_{10}C(CO)_{24}\}_2Hg]^{2-}} + PF_6^- \quad (3)$$

provides an alternative high-yield route to **4** and may find general application in the synthesis of high-nuclearity Hg-linked transition-metal clusters.

Reactions of the Tetrahydrido Cluster $[Os_{10}H_4(CO)_{24}]^{2-}$ **7** *with Mercury Electrophiles.*—In the light of the chemistry related to the carbido cluster **1**, as discussed above, it was of interest whether the synthesis of the analogous condensation products based on the cluster $[Os_{10}H_4(CO)_{24}]^{2-}$ **7**[21] was feasible. However, the different redox behaviour of **7** has so far prevented the development of general synthetic routes leading to mixed-metal hydrido clusters derived from this species. As was shown in an earlier cyclovoltammetric study of both **1** and **7**, the latter has a significantly lower half-wave potential for the redox couple with its radical monoanion $[Os_{10}H_4(CO)_{24}]^-$ (+0.35 V) **7a** than that of **1** (+0.70 V).[18] As a consequence, most reactions of mercury(II) salts with **7** lead to oxidation of the cluster along with the generation of metallic mercury. The reactions of **7** with $Hg(O_2CCF_3)_2$, $Hg(O_3SCF_3)_2$ and $Hg(CF_3)(O_2CCF_3)$ were studied in detail. For example, on treating the cluster with the trifluoroacetate a thermally unstable compound is generated initially which, based on the ν(CO) absorption band pattern of its infrared spectrum, is thought to be the analogue of **2g**, $[Os_{10}H_4(CO)_{24}(HgO_2CCF_3)]^-$ **8**. Within a period of *ca.* 10–15 h this cluster undergoes degradation to the aforementioned radical monoanion and Hg metal. We propose that this process probably occurs *via* the linked analogue of **4** (Scheme 1). This proposed

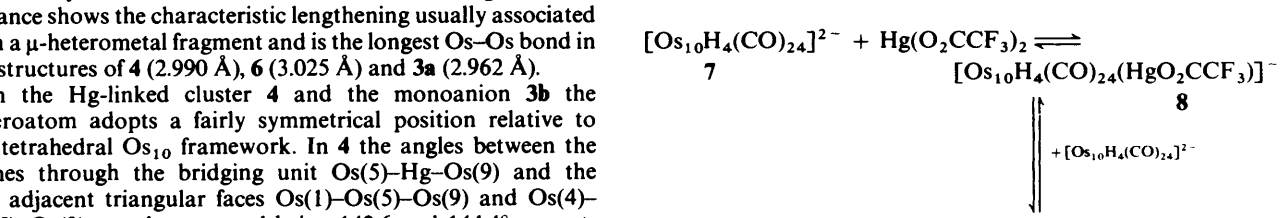

Scheme 1

pathway involving the short-lived Hg-linked species which could not be characterised is supported by two observations. The oxidation occurs instantaneously (reaction time < 1 min) if the triflate is used instead of the trifluoroacetate. Based on the well established chemistry of the carbido cluster, we know that this salt immediately generates **4**, the carbido analogue of the proposed intermediate. On the other hand, the reaction of **7** with $Hg(CF_3)(O_2CCF_3)$ generates the capped cluster $[Os_{10}H_4(CO)_{24}(HgCF_3)]^-$ **9** in which one co-ordination site on the Hg atom is blocked by the CF_3 group. This cluster proved to be stable in solution and is currently being studied in more detail.

Conclusion

The results of the reactivity studies based on the decaosmium cluster dianion $[Os_{10}C(CO)_{24}]^{2-}$ **1** are summarised in Scheme 2. We have shown that through careful selection of the mercury reagents it is possible to develop efficient preparative methods for a variety of standard structural types derived from **1**. While their solid-state structural features are now well understood, current (see following paper) and future investigations will focus on their dynamic behaviour in solution.

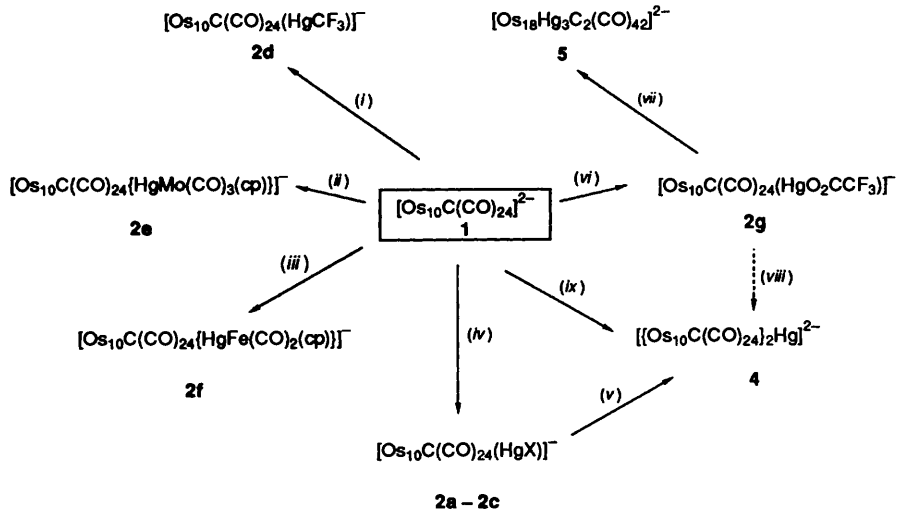

Scheme 2 Summary of the reactivity of $[Os_{10}C(CO)_{24}]^{2-}$ **1** towards mercury(II) electrophiles: (*i*) $+Hg(CF_3)(O_2CCF_3)$; (*ii*) + $[Mo(CO)_3(cp)(HgCl)]$–$TlPF_6$; (*iii*) + $[Fe(CO)_2(cp)(HgCl)]$–$TlPF_6$; (*iv*) + HgX_2 (X = Cl, Br or I); (*v*) + **1**–$TlPF_6$; (*vi*) + $Hg(O_2CCF_3)_2$; (*vii*) + 0.6 equivalent of $Hg(O_2CCF_3)_2$; (*viii*) + **1**; (*ix*) + 0.6 equivalent of $Hg(O_3SCF_3)_2$

Table 4 Crystal and X-ray structure analysis data *

Anion	**2b**	**2d**	**4**
Cation	$[N(PPh_3)_2]^+$	$[PPh_4]^+$	$[N(PPh_3)_2]^+$
Formula	$C_{61}H_{30}BrHgNO_{24}Os_{10}P_2$	$C_{50}H_{20}F_3HgO_{24}Os_{10}P$	$C_{122}H_{60}HgN_2O_{48}Os_{20}P_4$
M	3405.25	3194.67	6448.98
System	Triclinic	Triclinic	Monoclinic
Space group	$P\bar{1}$ (no. 2)	$P\bar{1}$ (no. 2)	$C2/c$ (no. 15)
a/Å	21.816(4)	15.986(3)	35.526(7)
b/Å	15.481(3)	11.865(3)	22.517(5)
c/Å	11.977(2)	17.471(4)	18.288(4)
α/°	102.16(3)	90.12(2)	90
β/°	103.97(3)	115.81(3)	104.76(2)
γ/°	93.33(2)	90.19(2)	90
U/Å^3	3806.2	2983.2	14 147
Z	2	2	4
D_c/g cm^{-3}	2.97	3.56	3.03
μ(Mo-Kα)/cm^{-1}	185.6	238.3	190.5
F(000)	3000	2788	11 400
Crystal size (10^2 mm)	40 × 35 × 28	35 × 13 × 2	37 × 6 × 5
No. unique data $[I/\sigma(I) \geqslant 3.0]$	7100	3451	3837
θ range/°	3–25	3–23	3–25
Anisotropic atoms	Br, Hg, Os, P	Hg, Os, P	Hg, Os, P
R	0.0590	0.0645	0.0489
R'	0.0609	0.0623	0.0470

* Details pertaining to all structures: Mo-Kα radiation, λ = 0.710 69 Å; unit-cell dimensions and data collection by methods described previously (ref. 28); Philips PW 1100 four-circle diffractometer; scan mode ω–2θ; central Os_6 octahedron location by Patterson, remaining non-hydrogen atoms from Fourier-difference syntheses; phenyl rings idealised (C–C 1.395, C–H 1.08 Å); empirical absorption correction (ref. 29); full-matrix least-squares refinement (ref. 30); weighting scheme $w = [\sigma^2(F_o)]^{-1}$. Final Fourier-difference syntheses showed no maximum above *ca.* 1 e Å^{-3} except in the vicinity of the metal atoms.

The limits of the synthetic methodology become apparent in systems like those derived from $[Os_{10}H_4(CO)_{24}]^{2-}$ in which the redox properties of the cluster prevents the build-up of stable systems with larger metal cores. Cluster redox chemistry will dominate the reactive behaviour of osmium clusters with a substantially larger nuclearity than 10, such as $[Os_{17}(CO)_{36}]^{2-}$ [23] and $[Os_{20}(CO)_{40}]^{2-}$ [24] which will therefore require a different chemical approach in studies on their reactivity.

Experimental

All manipulations were performed under an inert-gas atmosphere of dried argon in standard (Schlenk) glassware using canula/septa techniques. Solvents were dried according to standard procedures and saturated with Ar or N_2 prior to use. The ^{13}C NMR spectra were recorded on a Bruker AM400 spectrometer, IR spectra on Perkin-Elmer PE 983 and PE 1710 spectrometers and FAB mass spectra on KRATOS MS50 and MS890 spectrometers using 3-nitrobenzyl alcohol as matrix and CsI as calibrant. Simulations of the isotope distributions were carried out with a program implemented on the DS90 data system of the KRATOS MS890 mass spectrometer. The compounds $[N(PPh_3)_2]_2[Os_{10}C(CO)_{24}]$,[12b] $[N(PPh_3)_2]_2[Os_{10}H_4(CO)_{24}]$,[16] $Hg(O_3SCF_3)_2$[25] and $Hg(CF_3)(O_2CCF_3)$[26] were prepared as reported in the literature. Compounds used for ^{13}C NMR spectroscopy were *ca.* 50% ^{13}C-enriched and synthesised from

Table 5 Fractional atomic coordinates

Atom	*x*	*y*	*z*	Atom	*x*	*y*	*z*
(*a*) $[N(PPh_3)_2]^+$ salt of **2b**							
Os(1)	−0.345 79(6)	−0.004 75(9)	0.119 07(13)	O(82)	−0.105 8(12)	0.121 3(17)	0.540 2(25)
Os(2)	−0.271 79(5)	0.061 91(8)	−0.028 47(11)	C(91)	−0.167 4(21)	0.309 7(29)	0.480 7(42)
Os(3)	−0.218 27(5)	−0.017 42(8)	0.170 98(11)	O(91)	−0.170 8(13)	0.323 0(19)	0.584 4(27)
Os(4)	−0.260 13(6)	0.158 89(9)	0.235 36(12)	C(92)	−0.082 8(20)	0.365 1(27)	0.369 9(37)
Os(5)	−0.180 17(6)	0.134 50(8)	−0.131 24(11)	O(92)	−0.029 2(14)	0.402 2(19)	0.404 9(26)
Os(6)	−0.139 24(5)	0.046 23(8)	0.043 46(11)	C(93)	−0.199 1(19)	0.402 8(28)	0.305 0(38)
Os(7)	−0.084 48(6)	−0.029 35(8)	0.227 47(11)	O(93)	−0.223 0(13)	0.465 4(19)	0.288 8(26)
Os(8)	−0.128 31(6)	0.133 59(8)	0.282 34(11)	C(101)	−0.106 7(15)	0.284 9(20)	0.102 9(27)
Os(9)	−0.160 48(7)	0.303 04(9)	0.331 33(12)	O(101)	−0.056 1(12)	0.313 5(16)	0.105 5(22)
Os(10)	−0.181 31(6)	0.218 70(8)	0.095 92(11)	C(102)	−0.231 7(16)	0.307 8(23)	0.047 4(32)
Hg	−0.374 00(7)	0.145 45(11)	0.041 32(16)	O(102)	−0.266 6(12)	0.351 8(17)	0.011 9(23)
Br	−0.455 2(2)	0.237 3(4)	−0.028 9(5)	P(1)	0.321 4(4)	0.418 6(5)	0.335 3(8)
C	−0.203 7(14)	0.101 7(20)	0.133 0(27)	P(2)	0.348 7(4)	0.305 3(5)	0.509 9(7)
C(11)	−0.343 6(14)	−0.111 0(21)	0.171 9(28)	N	0.350 9(11)	0.346 9(15)	0.398 8(21)
O(11)	−0.344 7(10)	−0.172 1(15)	0.206 9(20)	C(111)	0.339 8(10)	0.398 9(14)	0.196 0(15)
C(12)	−0.412 2(25)	−0.051 3(36)	−0.015 4(50)	C(112)	0.319 6(10)	0.454 8(14)	0.120 1(15)
O(12)	−0.444 7(15)	−0.099 6(21)	−0.102 3(30)	C(113)	0.334 0(10)	0.441 1(14)	0.010 7(15)
C(13)	−0.401 0(22)	0.032 2(31)	0.209 6(44)	C(114)	0.368 6(10)	0.371 6(14)	−0.022 8(15)
O(13)	−0.433 8(15)	0.060 3(22)	0.272 6(30)	C(115)	0.388 8(10)	0.315 8(14)	0.053 1(15)
C(21)	−0.291 3(15)	−0.053 5(23)	−0.135 0(31)	C(116)	0.374 4(10)	0.329 5(14)	0.162 5(15)
O(21)	−0.303 2(11)	−0.120 7(17)	−0.187 9(23)	C(121)	0.357 4(10)	0.528 8(11)	0.410 7(19)
C(22)	−0.319 5(13)	0.107 0(19)	−0.151 6(26)	C(122)	0.327 1(10)	0.603 6(11)	0.393 1(19)
O(22)	−0.348 1(12)	0.134 8(17)	−0.233 5(24)	C(123)	0.358 2(10)	0.688 5(11)	0.449 5(19)
C(31)	−0.215 0(11)	−0.051 2(15)	0.315 5(21)	C(124)	0.419 6(10)	0.698 6(11)	0.523 6(19)
O(31)	−0.210 8(11)	−0.070 9(16)	0.405 3(23)	C(125)	0.449 9(10)	0.623 8(11)	0.541 1(19)
C(32)	−0.229 4(15)	−0.141 3(22)	0.083 1(30)	C(126)	0.418 8(10)	0.538 9(11)	0.484 7(19)
O(32)	−0.232 9(10)	−0.209 4(16)	0.031 5(21)	C(131)	0.238 1(7)	0.416 9(13)	0.314 4(17)
C(41)	−0.269 6(14)	0.133 0(19)	0.377 5(27)	C(132)	0.212 3(7)	0.461 5(13)	0.403 2(17)
O(41)	−0.271 4(12)	0.125 4(16)	0.471 0(23)	C(133)	0.146 9(7)	0.449 6(13)	0.390 5(17)
C(42)	−0.304 4(16)	0.255 7(23)	0.256 1(31)	C(134)	0.107 3(7)	0.393 1(13)	0.288 9(17)
O(42)	−0.328 9(16)	0.321 3(23)	0.283 9(31)	C(135)	0.133 1(7)	0.348 5(13)	0.200 0(17)
C(51)	−0.106 9(18)	0.184 6(24)	−0.153 8(33)	C(136)	0.198 5(7)	0.360 4(13)	0.212 8(17)
O(51)	−0.056 2(13)	0.194 6(17)	−0.177 9(24)	C(211)	0.377 7(10)	0.198 2(11)	0.482 0(19)
C(52)	−0.197 0(14)	0.040 9(20)	−0.271 1(28)	C(212)	0.425 2(10)	0.187 6(11)	0.422 1(19)
O(52)	−0.211 5(13)	−0.022 1(18)	−0.354 2(25)	C(213)	0.448 6(10)	0.105 5(11)	0.399 0(19)
C(53)	−0.218 2(15)	0.220 9(22)	−0.202 7(30)	C(214)	0.424 4(10)	0.034 0(11)	0.435 9(19)
O(53)	−0.244 3(12)	0.269 8(17)	−0.251 9(23)	C(215)	0.376 9(10)	0.044 7(11)	0.495 8(19)
C(61)	−0.057 4(15)	0.090 0(21)	0.043 8(28)	C(216)	0.353 5(10)	0.126 7(11)	0.518 9(19)
O(61)	−0.004 9(10)	0.106 9(14)	0.041 6(19)	C(221)	0.271 3(7)	0.285 5(14)	0.529 7(19)
C(62)	−0.142 3(13)	−0.059 8(19)	−0.069 2(26)	C(222)	0.256 5(7)	0.314 9(14)	0.637 6(19)
O(62)	−0.146 2(10)	−0.125 1(15)	−0.133 8(20)	C(223)	0.194 1(7)	0.300 4(14)	0.645 5(19)
C(71)	−0.085 9(14)	−0.147 5(20)	0.141 9(27)	C(224)	0.146 5(7)	0.256 5(14)	0.545 5(19)
O(71)	−0.087 4(11)	−0.217 5(16)	0.087 3(22)	C(225)	0.161 3(7)	0.227 1(14)	0.437 6(19)
C(72)	0.000 5(14)	−0.003 7(19)	0.246 4(25)	C(226)	0.223 7(7)	0.241 6(14)	0.429 7(19)
O(72)	0.052 4(11)	0.013 8(15)	0.245 1(21)	C(231)	0.399 6(9)	0.373 4(12)	0.644 3(15)
C(73)	−0.067 7(13)	−0.064 3(19)	0.373 7(26)	C(232)	0.383 1(9)	0.456 9(12)	0.689 3(15)
O(73)	−0.054 8(12)	−0.077 6(17)	0.466 3(24)	C(233)	0.424 9(9)	0.514 9(12)	0.786 8(15)
C(81)	−0.044 6(15)	0.180 1(20)	0.304 3(27)	C(234)	0.483 2(9)	0.489 3(12)	0.839 2(15)
O(81)	0.007 7(12)	0.212 0(17)	0.322 1(23)	C(235)	0.499 7(9)	0.405 7(12)	0.794 3(15)
C(82)	−0.116 9(16)	0.122 2(23)	0.437 7(33)	C(236)	0.457 9(9)	0.347 8(12)	0.696 8(15)
(*b*) The $[PPh_4]^+$ salt of **2d**							
Os(1)	−0.005 4(2)	0.200 0(2)	0.373 8(2)	O(21)	−0.275 8(36)	0.133 2(40)	0.373 7(33)
Os(2)	−0.208 7(2)	0.244 7(2)	0.253 6(2)	C(22)	−0.261 1(41)	0.374 4(48)	0.262 9(38)
Os(3)	−0.104 4(2)	0.042 4(2)	0.253 9(2)	O(22)	−0.295 7(38)	0.459 7(45)	0.278 8(36)
Os(4)	−0.047 5(2)	0.254 2(2)	0.204 3(2)	C(31)	−0.008 9(45)	−0.043 5(49)	0.269 2(40)
Os(5)	−0.389 6(2)	0.263 6(2)	0.110 7(2)	O(31)	0.063 4(31)	−0.098 1(35)	0.287 7(28)
Os(6)	−0.288 9(2)	0.071 1(2)	0.128 1(2)	C(32)	−0.142 9(40)	−0.043 5(45)	0.324 8(37)
Os(7)	−0.194 1(2)	−0.123 6(2)	0.125 9(2)	O(32)	−0.162 1(28)	−0.094 3(32)	0.376 4(26)
Os(8)	−0.138 2(2)	0.077 7(2)	0.083 2(2)	C(41)	0.069 3(45)	0.203 6(50)	0.233 0(40)
Os(9)	−0.092 4(2)	0.273 6(2)	0.028 9(2)	O(41)	0.149 5(36)	0.162 3(40)	0.252 5(32)
Os(10)	−0.236 0(2)	0.282 5(2)	0.078 8(2)	C(42)	−0.002 2(39)	0.403 4(45)	0.206 6(36)
Hg	−0.082 7(2)	0.413 8(2)	0.328 7(2)	O(42)	0.030 1(27)	0.487 1(31)	0.202 3(24)
C	−0.163 7(35)	0.164 1(39)	0.171 9(32)	C(51)	−0.490 7(50)	0.241 8(56)	0.001 9(47)
C(11)	0.087 1(62)	0.104 2(70)	0.419 5(56)	O(51)	−0.551 4(32)	0.226 1(36)	−0.062 4(30)
O(11)	0.154 8(37)	0.046 4(42)	0.443 1(33)	C(52)	−0.470 1(79)	0.226 3(89)	0.151 1(75)
C(12)	−0.036 2(45)	0.176 6(53)	0.465 0(43)	O(52)	−0.483 7(41)	0.192 9(48)	0.212 4(40)
O(12)	−0.053 6(32)	0.150 9(36)	0.519 4(30)	C(53)	−0.435 5(49)	0.412 9(59)	0.103 2(45)
C(13)	0.078 6(51)	0.314 8(57)	0.439 6(45)	O(53)	−0.448 3(37)	0.513 2(47)	0.092 1(35)
O(13)	0.149 7(44)	0.374 4(50)	0.463 5(40)	C(61)	−0.382 3(55)	0.021 6(61)	0.017 8(52)
C(21)	−0.240 8(41)	0.174 6(47)	0.327 4(38)				

Table 5 (*continued*)

Atom	*x*	*y*	*z*	Atom	*x*	*y*	*z*
(*b*) The $[PPh_4]^+$ salt of **2d**							
O(61)	−0.426 8(33)	−0.004 7(37)	−0.043 3(32)	F(3)	−0.106 9(47)	0.633 7(54)	0.387 8(42)
C(62)	−0.351 4(37)	−0.004 7(41)	0.182 7(34)	P	0.448 8(14)	0.249 6(16)	0.433 3(12)
O(62)	−0.376 7(27)	−0.060 3(30)	0.224 8(25)	C(111)	0.375 6(27)	0.343 2(35)	0.356 8(27)
C(71)	−0.239 4(39)	−0.223 7(45)	0.184 3(37)	C(112)	0.331 6(27)	0.431 9(35)	0.376 9(27)
O(71)	−0.254 4(33)	−0.287 7(39)	0.225 9(31)	C(113)	0.267 7(27)	0.498 5(35)	0.312 5(27)
C(72)	−0.270 0(48)	−0.188 6(55)	0.029 1(46)	C(114)	0.247 6(27)	0.476 4(35)	0.227 8(27)
O(72)	−0.303 4(31)	−0.229 7(35)	−0.037 7(29)	C(115)	0.291 5(27)	0.387 6(35)	0.207 6(27)
C(73)	−0.084 8(63)	−0.207 4(73)	0.161 5(57)	C(116)	0.355 5(27)	0.321 0(35)	0.272 1(27)
O(73)	−0.043 7(43)	−0.270 6(50)	0.144 4(39)	C(121)	0.434 1(37)	0.258 8(41)	0.529 3(26)
C(81)	−0.209 7(46)	0.038 1(52)	−0.033 8(44)	C(122)	0.355 3(37)	0.216 1(41)	0.534 4(26)
O(81)	−0.247 0(28)	−0.001 6(32)	−0.100 6(27)	C(123)	0.340 9(37)	0.237 4(41)	0.606 3(26)
C(82)	−0.031 3(39)	0.008 1(43)	0.087 5(34)	C(124)	0.405 4(37)	0.301 4(41)	0.673 2(26)
O(82)	0.046 4(32)	−0.026 7(36)	0.101 3(30)	C(125)	0.484 2(37)	0.344 1(41)	0.668 1(26)
C(91)	0.025 4(40)	0.252 2(44)	0.042 9(35)	C(126)	0.498 6(37)	0.322 8(41)	0.596 2(26)
O(91)	0.106 9(32)	0.229 6(35)	0.055 6(28)	C(131)	0.568 5(24)	0.283 8(36)	0.460 9(29)
C(92)	−0.144 5(36)	0.255 1(40)	−0.089 5(34)	C(132)	0.642 7(24)	0.223 7(36)	0.521 1(29)
O(92)	−0.177 9(30)	0.230 8(35)	−0.163 1(29)	C(133)	0.733 8(24)	0.257 8(36)	0.542 5(29)
C(93)	−0.092 7(45)	0.435 1(54)	0.013 4(42)	C(134)	0.750 7(24)	0.352 1(36)	0.503 7(29)
O(93)	−0.104 7(35)	0.526 3(43)	−0.004 2(33)	C(135)	0.676 5(24)	0.412 3(36)	0.443 4(29)
C(101)	−0.316 8(42)	0.276 5(46)	−0.037 4(39)	C(136)	0.585 4(24)	0.378 1(36)	0.422 0(29)
O(101)	−0.367 9(30)	0.279 2(34)	−0.106 2(29)	C(141)	0.429 1(33)	0.115 1(42)	0.389 4(32)
C(102)	−0.240 0(49)	0.452 3(59)	0.079 6(45)	C(142)	0.339 8(33)	0.070 1(42)	0.360 5(32)
O(102)	−0.251 1(44)	0.544 2(53)	0.099 7(42)	C(143)	0.315 5(33)	−0.027 1(42)	0.310 3(32)
C(1)	−0.053 6(74)	0.577 8(82)	0.373 1(68)	C(144)	0.380 5(33)	−0.079 3(42)	0.288 9(32)
F(1)	0.015 3(41)	0.596 9(45)	0.437 4(38)	C(145)	0.469 9(33)	−0.034 3(42)	0.317 7(32)
F(2)	−0.042 3(45)	0.654 4(56)	0.318 5(44)	C(146)	0.494 2(33)	0.062 9(42)	0.368 0(32)
(*c*) $[N(PPh_3)_2]^+$ salt of **4**							
Os(1)	0.451 25(5)	0.128 20(7)	0.493 42(9)	C(81)	0.444 1(15)	0.204 4(24)	0.253 2(32)
Os(2)	0.390 37(5)	0.198 19(7)	0.401 61(10)	O(81)	0.452 3(8)	0.240 8(13)	0.215 8(17)
Os(3)	0.466 10(5)	0.248 44(7)	0.457 01(9)	C(82)	0.427 9(13)	0.098 6(20)	0.283 3(26)
Os(4)	0.387 57(5)	0.169 37(7)	0.553 89(9)	O(82)	0.414 1(8)	0.057 5(12)	0.249 8(16)
Os(5)	0.465 99(5)	0.218 38(7)	0.610 37(9)	C(83)	0.501 5(12)	0.129 2(16)	0.349 3(22)
Os(6)	0.402 35(5)	0.288 02(7)	0.517 43(10)	O(83)	0.531 2(10)	0.113 4(14)	0.355 0(18)
Os(7)	0.475 27(5)	0.339 59(7)	0.560 16(10)	C(91)	0.414 6(13)	0.028 4(19)	0.596 7(25)
Os(8)	0.451 62(5)	0.159 70(7)	0.345 49(9)	O(91)	0.396 2(9)	−0.015 1(14)	0.577 5(18)
Os(9)	0.444 27(5)	0.092 99(7)	0.634 78(9)	C(92)	0.488 2(12)	0.041 2(18)	0.660 6(23)
Os(10)	0.329 18(5)	0.236 60(8)	0.455 40(11)	O(92)	0.512 3(9)	0.009 0(14)	0.665 3(18)
Hg	0.500 00	0.158 66(10)	0.750 00	C(93)	0.424 4(14)	0.089 9(21)	0.720 4(29)
C	0.426 5(9)	0.207 2(14)	0.507 1(19)	O(93)	0.415 8(8)	0.087 7(13)	0.775 9(18)
C(11)	0.502 0(12)	0.101 3(17)	0.508 3(22)	C(101)	0.292 3(13)	0.178 2(22)	0.418 8(27)
O(11)	0.532 9(10)	0.081 8(15)	0.524 5(20)	O(101)	0.272 4(10)	0.140 0(17)	0.393 5(22)
C(12)	0.428 2(13)	0.055 7(20)	0.448 1(26)	C(102)	0.305 3(20)	0.294 0(33)	0.380 6(26)
O(12)	0.413 8(9)	0.011 9(15)	0.421 4(19)	O(102)	0.289 8(16)	0.319 5(19)	0.331 8(30)
C(21)	0.360 4(12)	0.137 7(19)	0.349 5(25)	C(103)	0.299 7(26)	0.258 7(37)	0.519 1(65)
O(21)	0.340 4(9)	0.098 1(14)	0.320 0(18)	O(103)	0.290 0(11)	0.275 3(27)	0.575 1(29)
C(22)	0.376 3(11)	0.251 4(17)	0.317 8(22)	P(1)	0.278 6(3)	0.420 4(5)	0.065 3(7)
O(22)	0.367 9(8)	0.285 1(13)	0.272 9(18)	P(2)	0.329 3(3)	0.328 9(5)	0.019 4(7)
C(31)	0.518 4(12)	0.242 3(18)	0.459 0(25)	N	0.295 1(8)	0.357 5(13)	0.049 8(17)
O(31)	0.553 0(9)	0.237 0(12)	0.470 0(17)	C(111)	0.234 8(7)	0.410 0(14)	0.096 9(16)
C(32)	0.459 8(14)	0.307 2(22)	0.377 8(30)	C(112)	0.227 4(7)	0.354 6(14)	0.124 2(16)
O(32)	0.459 3(9)	0.342 9(16)	0.330 7(20)	C(113)	0.194 5(7)	0.346 2(14)	0.151 5(16)
C(41)	0.371 3(11)	0.190 4(16)	0.632 6(22)	C(114)	0.169 0(7)	0.393 4(14)	0.151 4(16)
O(41)	0.359 4(9)	0.198 5(14)	0.691 9(19)	C(115)	0.176 4(7)	0.448 9(14)	0.124 1(16)
C(42)	0.352 4(16)	0.110 0(25)	0.533 6(32)	C(116)	0.209 3(7)	0.457 2(14)	0.096 8(16)
O(42)	0.331 3(10)	0.067 5(15)	0.509 4(20)	C(121)	0.310 6(9)	0.459 6(16)	0.141 1(16)
C(51)	0.457 0(11)	0.264 1(16)	0.687 7(22)	C(122)	0.341 9(9)	0.428 1(16)	0.186 2(16)
O(51)	0.448 7(9)	0.296 4(13)	0.739 2(18)	C(123)	0.367 9(9)	0.456 5(16)	0.246 2(16)
C(52)	0.521 1(11)	0.216 8(16)	0.636 3(22)	C(124)	0.362 7(9)	0.516 3(16)	0.261 0(16)
O(52)	0.555 5(8)	0.212 6(12)	0.638 1(16)	C(125)	0.331 4(9)	0.547 7(16)	0.215 9(16)
C(61)	0.387 5(13)	0.352 2(21)	0.456 8(27)	C(126)	0.305 4(9)	0.519 4(16)	0.155 9(16)
O(61)	0.377 0(9)	0.391 8(15)	0.411 5(19)	C(131)	0.267 7(10)	0.466 5(14)	−0.014 7(16)
C(62)	0.383 7(15)	0.323 3(22)	0.591 0(31)	C(132)	0.232 2(10)	0.455 7(14)	−0.067 0(16)
O(62)	0.370 1(10)	0.343 3(16)	0.637 3(21)	C(133)	0.223 2(10)	0.484 8(14)	−0.136 6(16)
C(71)	0.473 0(13)	0.403 9(21)	0.494 7(27)	C(134)	0.249 7(10)	0.524 7(14)	−0.154 0(16)
O(71)	0.468 9(9)	0.445 6(14)	0.456 1(19)	C(135)	0.285 1(10)	0.535 6(14)	−0.101 7(16)
O(72)	0.464 9(14)	0.390 4(22)	0.635 0(29)	C(136)	0.294 1(10)	0.506 5(14)	−0.032 1(16)
O(72)	0.461 6(12)	0.421 2(19)	0.680 7(25)	C(211)	0.337 1(8)	0.256 0(10)	0.054 6(15)
C(73)	0.529 8(14)	0.351 3(20)	0.590 8(26)	C(212)	0.320 7(8)	0.238 7(10)	0.112 9(15)
O(73)	0.563 6(10)	0.355 0(16)	0.615 3(20)	C(213)	0.327 8(8)	0.182 0(10)	0.144 0(15)

Table 5 (*continued*)

Atom	*x*	*y*	*z*	Atom	*x*	*y*	*z*
(*c*) $[N(PPh_3)_2]^+$ salt of **4**							
C(214)	0.351 4(8)	0.142 6(10)	0.116 9(15)	C(226)	0.378 6(8)	0.419 3(13)	0.007 4(18)
C(215)	0.367 8(8)	0.159 8(10)	0.058 6(15)	C(231)	0.317 0(9)	0.322 9(13)	−0.079 2(14)
C(216)	0.360 7(8)	0.216 5(10)	0.027 4(15)	C(232)	0.278 1(9)	0.321 0(13)	−0.120 2(14)
C(221)	0.374 8(8)	0.367 9(13)	0.047 7(18)	C(233)	0.268 7(9)	0.312 2(13)	−0.198 3(14)
C(222)	0.404 5(8)	0.351 4(13)	0.110 2(18)	C(234)	0.298 2(9)	0.305 2(13)	−0.235 3(14)
C(223)	0.438 0(8)	0.386 3(13)	0.132 6(18)	C(235)	0.337 1(9)	0.307 1(13)	−0.194 4(14)
C(224)	0.441 7(8)	0.437 6(13)	0.092 3(18)	C(236)	0.346 5(9)	0.316 0(13)	−0.116 3(14)
C(225)	0.412 0(8)	0.454 2(13)	0.029 8(18)				

enriched $[Os_3(CO)_{12}]$ which was obtained as described in ref. 27.

Preparation of Compounds.—$[N(PPh_3)_2][Os_{10}C(CO)_{24}(HgBr)]$ **2b**. The compound $[N(PPh_3)_2]_2[Os_{10}C(CO)_{24}]$ (50 mg, 0.0136 mmol) was dissolved in CH_2Cl_2 (20 cm^3). To this solution was added solid $HgBr_2$ (6 mg, 0.0166 mmol, 1.2 equivalents). The reaction was monitored by IR spectroscopy which showed complete conversion into **2b** after 10 min. The solvent volume was then reduced to 10 cm^3, layered with diethyl ether and the product crystallised at room temperature within *ca.* 10 h; 38 mg (82%) of crystalline material, some of it suitable for X-ray crystallography, were obtained.

The reactions with $HgCl_2$ and HgI_2 were carried out in the same way and the products precipitated with pentane to yield *ca.* 60% $[N(PPh_3)_2][Os_{10}C(CO)_{24}(HgCl)]$ (containing impurities of **4** and **5** and 85% of $[N(PPh_3)_2][Os_{10}C(CO)_{24}(HgI)]$ respectively.

$[N(PPh_3)_2][Os_{10}C(CO)_{24}(HgCF_3)]$ **2d**. The compound $[N(PPh_3)_2]_2[Os_{10}C(CO)_{24}]$ (50 mg, 0.0136 mmol) was dissolved in CH_2Cl_2 (20 cm^3). To this solution was added solid $Hg(CF_3)(O_2CCF_3)$ (6.3 mg, 0.0164 mmol, 1.2 equivalents). The reaction was monitored by IR spectroscopy which showed complete conversion into **2d** after 5 min. The solvent volume was then reduced to 10 cm^3 and the reaction mixture slowly cooled to 25 °C. The product crystallised as black plates (yield of crystalline material 29.5 mg, 64%). Analogous reactions were performed with $[AsPh_4]^+$, $[PPh_4]^+$ and $[PMePh_3]^+$ salts of **1**. Crystals suitable for X-ray crystallography were obtained from the $[PPh_4]^+$ salt.

$[N(PPh_3)_2][Os_{10}C(CO)_{24}\{HgMo(CO)_3(cp)\}]$ **2e**. To $[N(PPh_3)_2]_2[Os_{10}C(CO)_{24}]$ **1** (50 mg, 0.0136 mmol), $TlPF_6$ (5.0 mg) and $[Mo(CO)_3(cp)(HgCl)]$ (6.6 mg, 0.0137 mmol) was added CH_2Cl_2 (20 cm^3). The reaction mixture was stirred for 2 h at room temperature after which complete conversion into **2e** had taken place, as judged by IR spectroscopy. The solution was filtered, the solvent volume reduced to 10 cm^3, the system layered with pentane (10 cm^3) and then stored at +4 °C. Within a period of *ca.* 3 d **2e** precipitated as a microcrystalline solid. Yield: 31.5 mg (64%) (Found: C, 23.80; H, 1.05; N, 0.50. Calc. for $C_{69}H_{35}HgMoNO_{27}Os_{10}P_2$: C, 23.20; H, 1.00; N, 0.40%).

$[N(PPh_3)_2][Os_{10}C(CO)_{24}\{HgFe(CO)_2(cp)\}]$ **2f**. To $[N(PPh_3)_2]_2[Os_{10}C(CO)_{24}]$ **1** (50 mg, 0.0136 mmol), $TlPF_6$ (5.0 mg), and $[Fe(CO)_2(cp)(HgCl)]$ (6.0 mg, 0.0145 mmol) was added CH_2Cl_2 (20 cm^3). The reaction mixture was stirred for 2 h at room temperature after which complete conversion into **2f** had taken place, as judged by IR spectroscopy. The solution was filtered, the system layered with pentane (10 cm^3) and then stored at −25 °C. Within a period of *ca.* 24 h **2f** precipitated as a microcrystalline solid. Yield: 24.5 mg (51%) (Found: C, 23.40; H, 1.10; N, 0.50. Calc. for $C_{68}H_{35}FeHgNO_{26}Os_{10}P_2$: C, 23.30; H, 1.00; N, 0.40%). The compound decomposed in solution at room temperature over a period of hours but could be stored in a deep-freeze without significant degradation for up to 1 week.

$[N(PPh_3)_2]_2[\{Os_{10}C(CO)_{24}\}_2Hg]$ **4**. (*a*) Compound **1** (100 mg, 0.0273 mmol) was dissolved in CH_2Cl_2 (30 cm^3) and solid $Hg(O_3SCF_3)_2$ (8.2 mg, 0.0164 mmol, 0.6 equivalent) added. Conversion into the reaction product was complete after 15 min. The solvent volume was then reduced to 15 cm^3 and the product crystallised at room temperature by vapour diffusion with diethyl ether. The brown-black crystal needles (74.0 mg, 84%) were suitable for X-ray crystallography.

(*b*) Compound **2b** (40 mg, 0.012 mmol), **1** (43 mg) and $TlPF_6$ (10 mg, two-fold excess) were dissolved in CH_2Cl_2 (20 cm^3). After stirring the reaction mixture for 30 min a complete conversion into the mercury-linked cluster was achieved as judged by IR spectroscopy.

Degradation of Compounds **2a**–**2c** *and* **2e** *in solution. The mercury-capped clusters* **2a**–**2c** and **2e** (20 mg) were dissolved in CH_2Cl_2 (20 cm^3) and the systems monitored by IR spectroscopy over a period of 6 weeks. By that time no further spectral changes were observed. While **4** and, with minor decomposition, **5** could be isolated by TLC (silica gel) with exclusion of light and therefore weighed and additionally characterised by mass spectrometry, the starting material remaining in solution was immediately 'decapped' on exposure to silica, regenerating **1**. The amount of **1** and **2a**–**2c**, **2e** could therefore only be estimated on the basis of the IR spectra obtained for the reaction mixture.

$[N(PPh_3)_2][Os_{10}H_4(CO)_{24}(HgCF_3)]$ **9**. The compound $[N(PPh_3)_2]_2[Os_{10}H_4(CO)_{24}]$ (50 mg, 0.0136 mmol) was dissolved in CH_2Cl_2 (20 cm^3). To this solution was added solid $Hg(CF_3)(O_2CCF_3)$ (6.3 mg, 0.0164 mmol, 1.2 equivalents). The reaction was monitored by IR spectroscopy which showed complete conversion into **9** after 5 min. The reaction product was precipitated as a black microcrystalline material with diethyl ether (Found: C, 21.80; H, 1.20; N, 0.40. Calc. for $C_{61}H_{34}F_3HgNO_{24}Os_{10}P_2$: C, 21.60; H, 1.10; N, 0.40%).

X-ray Structure Analyses of Compounds **2b**, **2d** *and* **4**.—Details of the data collection and structure solution are given in Table 4. Crystals of the $[PPh_4]^+$ salt of **2d** and the $[N(PPh_3)_2]^+$ salt of **4** were obtained with difficulty and diffracted weakly. The dianion **4** has exact crystallographic C_2 symmetry with the Hg atoms lying on a symmetry axis of the space group. The bromine atom in **2b** has relatively high thermal parameters possibly due to a small component of unresolved disorder at this site. The final atomic coordinates for the three structures are listed in Table 5.

Additional material available from the Cambridge Crystallographic Data Centre comprises H-atom coordinates, thermal parameters and remaining bond lengths and angles.

Acknowledgements

L. H. G. gratefully acknowledges the award of a Ph.D. scholarship by the Studientstiftung des deutschen Volkes and financial support by ICI plc. H. R. P. thanks the SERC for a postdoctoral research fellowship.

References

1 M. D. Vargas and J. N. Nicholls, *Adv. Inorg. Chem. Radiochem.*, 1986, **30**, 123.

2 J. S. Bradley and G. W. Hill, *U.S. Pat.* 4301086. 1981; A. Albinati, K. H. Dahmen, A. Togni and L. M. Venanzi, *Angew. Chem., Int. Ed. Engl.*, 1985, **24**, 766; M. F. Hallam, D. M. P. Mingos, T. Adatia and M. McPartlin, *J. Chem. Soc., Dalton Trans.*, 1988, 335; M. Fajardo, H. D. Holden, B. F. G. Johnson, J. Lewis and P. R. Raithby, *J. Chem. Soc., Chem. Commun.*, 1984, 24; G. Doyle, K. A. Ericksen and D. van Engen, *J. Chem. Soc., Chem. Commun.*, 1986, 445
3 C. E. Housecroft, A. L. Rheingold and M. S. Shongwe, *Organometallics*, 1989, **8**, 2651; C. P. Horwitz, E. M. Holt, C. P. Brock, and D. F. Shriver, *J. Am. Chem. Soc.*, 1985, **107**, 8136; I. D. Salter, *Adv. Organomet. Chem.*, 1989, **29**, 249.
4 B. F. G. Johnson, J. Lewis, W. J. H. Nelson, P. R. Raithby and M. D. Vargas, *J. Chem. Soc., Chem. Commun.*, 1983, 608.
5 R. S. Nyholm and K. Vrieze, *Proc. Chem. Soc.*, 1963, 138; *Chem. Ind. (London)*, 1964, 318; J. Lewis and S. B. Wild, *J. Chem. Soc. A*, 1966, 69.
6 (*a*) P. Braunstein, J. Rosé, A. Tiripicchio and M. Tiripicchio-Camellini, *Angew. Chem., Int. Ed. Engl.*, 1985, **24**, 767; (*b*) J. A. Iggo and M. J. Mays, *J. Chem. Soc., Dalton Trans.*, 1984, 643; (*c*) R. Fahmy, K. King, E. Rosenberg, A. Tiripicchio and M. Tiripicchio-Camellini, *J. Am. Chem. Soc.*, 1980, **102**, 3626; (*d*) P. Braunstein, J. Rosé, A. Tiripicchio and M. Tiripicchio-Camellini, *J. Chem. Soc., Chem. Commun.*, 1984, 391.
7 L. J. Farrugia, *J. Chem. Soc., Chem. Commun.*, 1987, 147.
8 B. F. G. Johnson, W. L. Kwik, J. Lewis, P. R. Raithby and V. P. Saharan, *J. Chem. Soc., Dalton Trans.*, 1991, 1037.
9 Y. Yamamoto, H. Yamazaki and T. Sakurai, *J. Am. Chem. Soc.*, 1982, **104**, 2329.
10 A. Albinati, A. Moor, P. S. Pregosin and L. M. Venanzi, *J. Am. Chem. Soc.*, 1982, **104**, 7672.
11 E. Rosenberg, D. Ryckman, I-Nan Hsu and R. W. Gellert, *Inorg. Chem.*, 1986, **25**, 194.
12 (*a*) P. F. Jackson, B. F. G. Johnson, J. Lewis, M. McPartlin and W. J. H. Nelson, *J. Chem. Soc., Chem. Commun.*, 1980, 224; (*b*) P. F. Jackson, B. F. G. Johnson, J. Lewis, W. J. H. Nelson and M. McPartlin, *J. Chem. Soc., Dalton Trans.*, 1982, 2099.
13 B. F. G. Johnson, J. Lewis, W. J. H. Nelson, M. D. Vargas, D. Braga and M. McPartlin, *J. Organomet. Chem.*, 1983, **246**, C69.
14 V. Dearing, S. R. Drake, B. F. G. Johnson, J. Lewis, M. McPartlin and H. R. Powell, *J. Chem. Soc., Chem. Commun.*, 1988, 1331.
15 L. H. Gade, B. F. G. Johnson, J. Lewis, M. McPartlin and H. R. Powell, *J. Chem. Soc., Chem. Commun.*, 1990, 110.
16 L. H. Gade, B. F. G. Johnson and J. Lewis, following paper.
17 D. Braga, B. F. G. Johnson, J. Lewis, M. McPartlin, W. J. H. Nelson and M. D. Vargas, *J. Chem. Soc., Chem. Commun.*, 1983, 241; A. Bashall, L. H. Gade, B. F. G. Johnson, J. Lewis, G. McIntyre and M. McPartlin, *Angew. Chem., Int. Ed. Engl.*, 1991, in the press.
18 S. R. Drake, B. F. G. Johnson, J. Lewis and R. C. S. McQueen, *J. Chem. Soc., Chem. Commun.*, 1987, 1051.
19 S. Ermer, K. King, K. L. Hardcastle, E. Rosenberg, A. M. M. Lanfredi, A. Tiripicchio and M. Tiripicchio-Camellini, *Inorg. Chem.*, 1983, **22**, 1339.
20 J. Wang, M. Sabat, C. P. Horwitz and D. F. Shriver, *Inorg. Chem.*, 1988, **27**, 552.
21 L. H. Gade, B. F. G. Johnson, J. Lewis, M. McPartlin, T. Kotch and A. J. Lees, *J. Am. Chem. Soc.*, 1991, **113**, 8698.
22 (*a*) M. P. Gomez-Sal, B. F. G. Johnson, J. Lewis, P. R. Raithby and S. N. A. B. Syed-Mustaffa, *J. Organomet. Chem.*, 1984, **272**, C21; (*b*) E. Rosenberg, K. L. Hardcastle, M. W. Day, R. Gobetto, S. Hajela and R. Muftikian, *Organometallics*, 1991, **10**, 203.
23 E. Charalambous, L. H. Gade, B. F. G. Johnson, J. Lewis, M. McPartlin and H. R. Powell, *J. Chem. Soc., Chem. Commun.*, 1990, 688.
24 A. J. Amoroso, L. H. Gade, B. F. G. Johnson, J. Lewis, P. R. Raithby and W.-T. Wong, *Angew. Chem., Int. Ed. Engl.*, 1991, **30**, 107.
25 W. G. Jackson, G. A. Lawrance, P. A. Lay and A. M. Sargeson, *Aust. J. Chem.*, 1982, **35**, 1561.
26 D. Seyferth, S. P. Hopper and G. J. Murphy, *J. Organomet. Chem.*, 1972, **46**, 201.
27 L. R. Martin, F. W. B. Einstein and R. K. Pomeroy, *Organometallics*, 1988, **7**, 294.
28 M. K. Cooper, P. J. Guerney and M. McPartlin, *J. Chem. Soc., Dalton Trans.*, 1982, 757.
29 N. Walker and D. Stuart, *Acta Crystallogr., Sect. A*, 1983, **39**, 158.
30 G. M. Sheldrick, SHELX 76, Crystal Structure Solving Package, Cambridge University, 1976.

Received 17*th September* 1991; *Paper* 1/04806F